Original Article

Journal of POWER AND ENERGY

Proc IMechE Part A:
J Power and Energy
0(0) 1–11

DOI: 10.1177/0957650919847920
journals.sagepub.com/home/pia

Strategy on performance improvement of inverse Brayton cycle system for energy recovery in turbocharged diesel engines

Dengting Zhu, Yun Lin and Xinqian Zheng

Abstract

The inverse Brayton cycle is a potential technology for waste heat energy recovery. It consists of three components: one turbine, one heat exchanger, and one compressor. The exhaust gas is further expanded to subatmospheric pressure in the turbine, and then cooled in the heat exchanger, last compressed in the compressor into the atmosphere. The process above is the reverse of the pressurized Brayton cycle. This work has presented the strategy on performance improvement of the inverse Brayton cycle system for energy recovery in turbocharged diesel engines, which has pointed the way to the future development of the inverse Brayton cycle system. In the paper, an experiment was presented to validate the numerical model of a 2.0 l turbocharged diesel engine. Meanwhile, the influence laws of the inverse Brayton cycle system critical parameters, including turbocharger speed and efficiencies, and heat exchanger efficiency, on the system performance improvement for energy recovery are explored at various engine operations. The results have shown that the engine exhaust energy recovery efficiency increases with the engine speed up, and it has a maximum increment of 6.1% at the engine speed of 4000 r/min (the engine rated power point) and the full load. At the moment, the absolute pressure was before final compression is 51.9 kPa. For the inverse Brayton cycle system development in the future, it is essential to choose a more effective heat exchanger. Moreover, variable geometry turbines are very appropriate to achieve a proper matching between the turbocharging system and the inverse Brayton cycle system.

Keywords

Inverse Brayton cycle, diesel engine, energy recovery, strategy

Date received: 21 August 2018; accepted: 25 February 2019

Introduction

Internal combustion engines (ICEs) are widely used and play a significant role in the industry. With energy shortages and environmental problems being of more and more concern, energy conservation and emission reduction are very important and urgent.[1,2] The scientific and public awareness of the environment and energy issues has generated great interests in the research of advanced technologies, especially in efficient ICEs.[3,4] From an energy balance perspective, approximately 30–45% of the fuel burned in such vehicles is released into the atmosphere as exhaust.[5] Therefore, recovery of a significant portion of this wasted energy would be highly advantageous by many potential technologies which mainly include thermoelectric generators (TEGs), organic Rankine cycle (ORC), turbocharging technology, and inverse Brayton cycle (IBC).[6]

TEGs allow lost thermal energy to be recovered, energy to be produced in extreme environments, electric power to be generated.[7] Compared to the traditional power generation systems, TEGs have their characteristics such as simple structure, high reliability, operate without any noise or vibration, and waste generation.[8,9] Kim and Kim[10] used steady-state engine experiments to study energy recovery. The results suggested that the contribution of the TEG system to energy increased from 1.54 to 1.68%. Jaworski et al.[11] made an experimental setup for TEGs and proved that phase change materials could be effectively used as both the heat sink and heat source. However, low generation power and large thickness restrict their usages. Another challenge is

Turbomachinery Laboratory, State Key Laboratory of Automotive Safety and Energy, Tsinghua University, Beijing, China

Corresponding author:
Xinqian Zheng, Turbomachinery Laboratory, State Key Laboratory of Automotive Safety and Energy, Tsinghua University, Beijing 100084, China.
Email: zhengxq@tsinghua.edu.cn

larger radiators and expansion pipes to exhaust manifolds. The size and weight of an automotive car radiator could be reduced without affecting its heat transfer performance by using nanofluid.[12,13]

ORC is commonly accepted as a viable technology to convert low to medium exergy heat sources into electricity.[14,15] The working fluid and expander selection strongly influence efficiency. Chen et al.[16] had an experimental study under 35 different working conditions. It could be pointed out that for other operating conditions and different working fluids, the best working fluid with the maximum efficiency cycle might not be the same. Dolz et al.[17] experimentally investigated different bottoming Rankine cycles with water–steam and ORC configurations, and analyzed additional innovative setups in a heavy-duty diesel engine to fit this engine with ORCs. However, the implementation of a cost-effective ORC deployment is proved to be hindered by several key factors, including the disjointing between the parameters considered in the simulation study and the parameters proved by the experiment, the use of low level ORC practices in advanced applications, and the challenge of integrating multiple heat recovery sources.[18,19]

Turbocharging technology is a well-accepted way to enhance the intake density by utilizing the waste gas energy.[20] Nowadays, it is applied to almost all diesel engines, and it makes possible for spark ignition (SI) engines downsizing through reducing pump work. Variable geometry turbines (VGTs) and two-stage turbochargers are the two mature technologies.[21,22] VGTs can offer enough exhaust pressure to drive exhaust gas recirculation (EGR) and allow air charge flow into the combustor properly by changing the throat area of the turbine.[23] A turbocharged engine with VGT has a small movable blade to guide the incoming exhaust air through the turbine blades. In different speed ranges, the angle of the blade will change to optimize exhaust gas flow for EGR.[24] Meanwhile, the two-stage turbocharging can provide high intake manifold pressure and improve transient behavior, because a smaller turbocharger is selected as a high pressure turbocharger, and two turbochargers can work together at low loads.[25] Compared with the single-stage turbocharging, the two-stage turbocharging provides flexibility to meet engine requirements at both low and high speeds because of load split. Usually, the exhaust gas emitted into the atmosphere in turbocharged engines also has much energy, especially at the high-speed range. The IBC system is acceptable for higher energy recovery rates.

IBC is considered as a potential exhaust-gas heat-recovery technology.[26] Wilson[27] proposed and explained the IBC which consisted of inversed entirely processes compared with the traditional Brayton cycle (BC).[27] A schematic diagram of a single-stage IBC system is presented in Figure 1. It can be seen that the IBC system mainly consists of three components: a turbine, a heat exchanger, and a compressor. The primary processes of the IBC system are performed as below.[28,29]

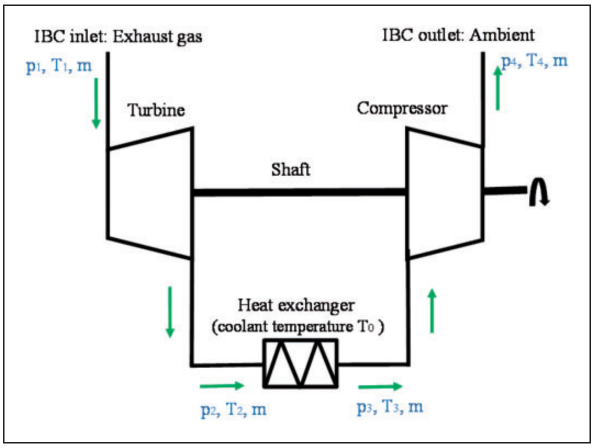

Figure 1. A schematic of single-stage IBC system.
IBC: inverse Brayton cycle.

First, the exhaust gas is further expanded in the IBC turbine to below environmental pressure. On the one hand, the power of the turbine is partially utilized for compression work in the compressor, and on the other hand, if the turbine has the mechanical energy left over, it can be exported by a shaft. Then, the heat exchanger cools the exhaust gas from the turbine, which is beneficial to reduce the energy consumption of the compressor. Finally, the exhaust gas is boosted to the environmental pressure by the compressor.

Zhang et al.[30] established a thermodynamic model for open combined BC and IBC considering the pressure drops of the working fluid along the flow processes, and the power output had a maximum concerning the compressor inlet pressure of the bottom cycle. The regenerated BC and IBC were reformed by partially passing the air stream entering the regenerator. The results presented that, from the point of view, a more favorable output power could be produced by adjusting the mass flow ratio of the bypass, and the thermal efficiency was reasonable.[31] Moreover, Giannetti et al.[32] proposed cascade refrigeration system at the cold end. The system configuration showed that the coefficient of performance was 50% higher than that of the corresponding simple BC at the refrigeration temperature of $-50\,^{\circ}$C. The IBC is a little-studied approach when applied to automotive power plants. A one-dimensional model of a small SI engine is verified, which is used as a baseline model for improving IBC performance.[33,34] The intake condition of IBC is different when the engine speed is limited.[35]

The IBC system is a potential and effective way to improve the recovery rate of exhaust energy. This work has pointed the strategy on performance improvement of the IBC system for energy recovery, which is very significant for the IBC system future development, and is not available in the public literature. Three parts consist in the paper. First, a turbocharged diesel engine experiment is performed, and the numerical models are established and validated. Second, the IBC system main parameters influence laws on engine performances are investigated. Finally, the strategy of improving system energy recovery rate is explored.

Experiment and simulation methods

In this study, an inline four-cylinder direct injection diesel engine equipped with a turbocharger is adopted on the dynamometer test bench. Details of the engine specifications are given in Table 1. AGW300 eddy current dynamometer with an accuracy of ±0.4% is used for engine speed and load management. An FC2212L type fuel consumption measuring instrument, with a precision of 0.12% of the recorded value, is applied to estimate the fuel consumption of the engine, and its measuring range is 0–75 kg/h. The intercooler component is FC2490, and the coolant has constant temperature regulated by an FC2422T control device (accuracy: ± 2 °C). The engine intake gas is collected by a 20N080 air flow meter whose measuring range is 0–800 kg/h, and the precision is ±1%. Moreover, the intake gas conditions are controlled by an air conditioning unit TOCEILZYAY-02 with the temperature and humidity adjusting accuracies of ±0.5 °C and 3%, respectively. The data acquisition system is an FC2022 instrument with the channel for collection of 2×16. In the experiment, the measuring and controlling device is FC2010, and the testing software is FC2005.

Based on the experiment, the numerical engine model is established with GT-POWER v7.3.0 software, which is frequently used in engine cycle simulations.[36] The pipes are modeled according to the experimental pipes shape and length, and the friction and heat transfer multipliers are within a reasonable range in reference to experimental pipes materials. In the combustor, the heat transfer model chooses the Woschni Formula. The experimental engine operating conditions are presented in Table 2, and these conditions were entirely adopted in the numerical models.

The study has compared the experimental and simulation results for the model validation. The maximum errors of the engine critical parameters (engine output torque, power, and brake-specific fuel consumption) between the simulated and experimental results are presented in Table 3. It can be seen that all the maximum errors are within 2.0%. There is only a low deviation between the experiment and emulation results. Therefore, for this research, the deviations are considered to be acceptable.

The four-cylinder diesel engine with an IBC system is presented in Figure 2(a). It can be seen that the IBC system is installed after the original turbine in the direction of exhaust gas flow. The engine exhaust gas

Table 1. Test engine specifications.

Items	Value and unit
Engine type	Inline 4-cylinder DI diesel
Number of valves per cylinder	4 (2 inlet/2 exhaust)
Bore	83 mm
Stroke	92 mm
Displacement	1991 cm^3
Compression ratio	17.5:1
Cooling system	Water cooled
Air intake system	Intercooled turbocharger
Rated power	110 kW (4000 r/min)
Maximum torque	310 N m (2000 r/min)

DI: direct injection.

Table 3. Maximum error between the simulated and experimental results.

Parameters	Maximum error (%)
Torque	1.96
Power	1.89
BSFC	1.98

BSFC: brake-specific fuel consumption.

Table 2. Experimental engine operating conditions.

Speed (r/min)	Power (kW)	Intake mass flow (kg/h)	Pre-intercooling pressure (kPa)	Fuel mass (kg/h)
4000	108.1	494	236.5	24.74
3600	107.3	455	234.5	23.32
3000	98.2	403	236.5	19.58
2600	87.0	352	237.5	16.71
2000	60.5	232	228.2	11.50
1600	48.1	161	194.2	9.91
1000	17.0	61	113.7	3.75

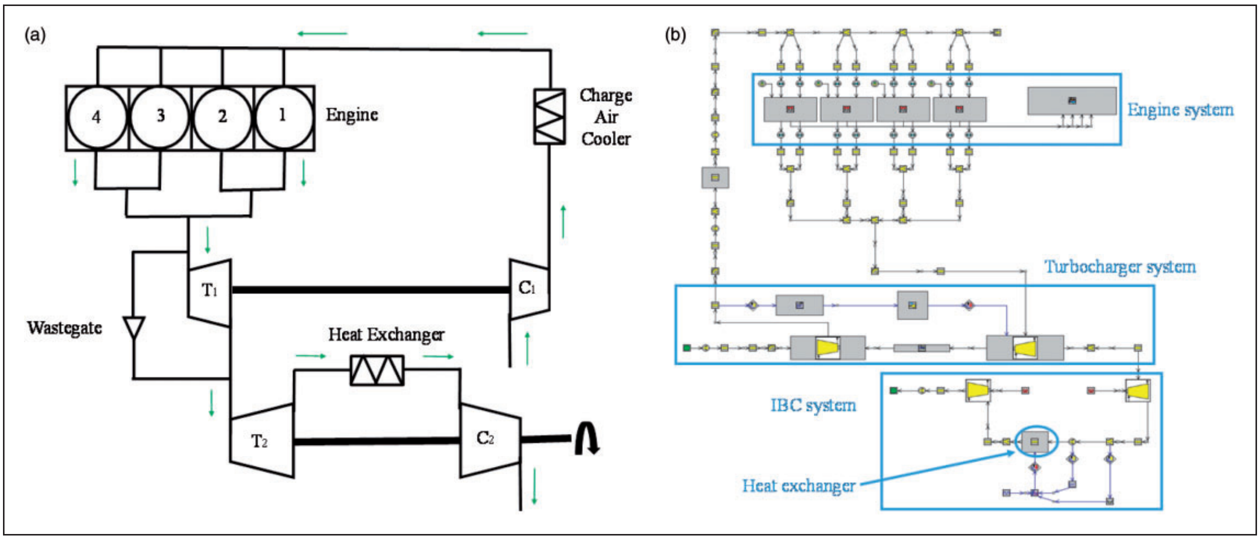

Figure 2. A four-cylinder diesel engine with an IBC system: (a) the schematic diagram and (b) the simulation model. IBC: inverse Brayton cycle.

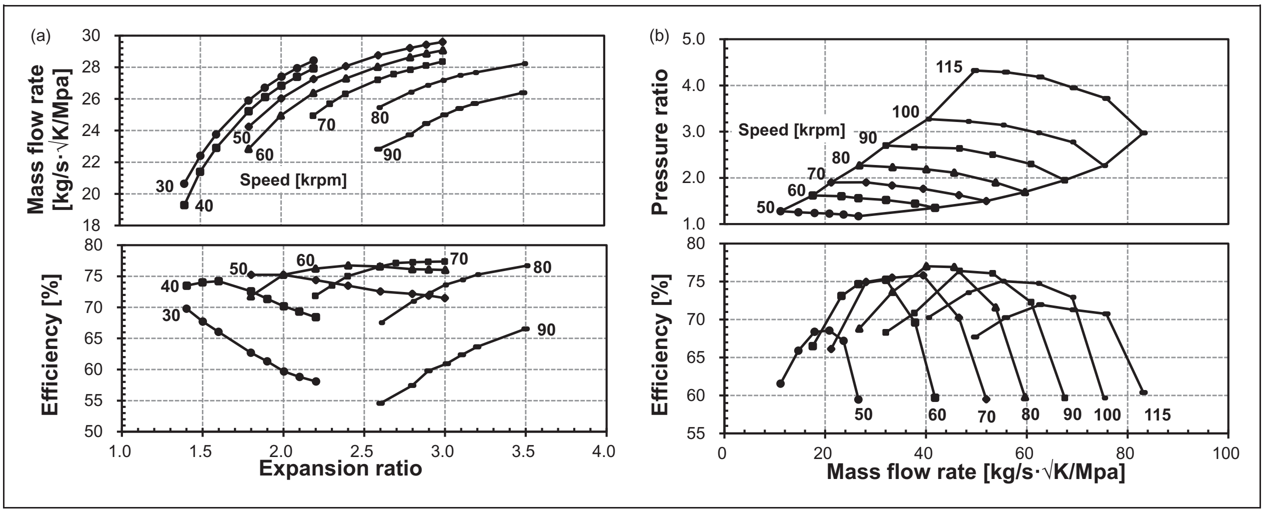

Figure 3. Turbocharger maps of the IBC system: (a) turbine map and (b) compressor map.

through the original turbine also has much energy, and some exhaust gas will directly go into the IBC system through the wastegate beyond the maximum torque point. As a consequence, the IBC system can further enhance the energy utilization. The GT-POWER model of the experimental turbocharged diesel engine with an IBC system is established as shown in Figure 2(b). Notably, the original turbocharged engine model remains unchanged, and the IBC turbine and compressor maps which are obtained from turbocharger experiments are shown in Figure 3.

Critical parameters influence laws

For the IBC system, the vital parameters including the compressor pressure ratio and efficiency, the turbine expansion ratio and efficiency, and the heat exchanger efficiency are essential. In this section, the engine cycle simulations are investigated to determine the influence laws of the crucial parameters on engine performances.

Turbocharger speed

In the IBC system, the turbine and the compressor have the same rotating speed by a shaft connection. The compressor pressure ratio and the turbine expansion ratio depend on the rotating speed. In the model of Figure 2(b), only the turbocharger speed is changed, and the power improvement of the IBC system which is defined as equation (1) is contained in Figure 4

$$\text{Power improvement} = \frac{(W_t - W_c)\eta_m}{W_e} \times 100\% \quad (1)$$

where W_e is the engine power, W_t is the turbine output power, W_c is the compressor compression power, η_m is the shaft mechanical efficiency and assumed 95% in the models. The power improvement can evaluate the capability of the waste gas energy recovery using the IBC system.

In the paper, the relative engine speed (RES) is dimensionless to the maximum engine speed at the full load (4000 r/min) as shown in equation (2) for a more concise expression

$$\mathrm{RES} = \frac{\text{Engine speed}}{4000\,\mathrm{r/min}} \times 100\% \tag{2}$$

In Figure 4, at engine full load operation, it can be seen that the power performance is better at the medium turbocharger speed and the maximum power improvement is 6.1% at 100% RES. At the moment, the absolute pressure before final compression is 51.9 kPa, and the compression ratio of the IBC compressor is 1.95. A higher power improvement means a bigger difference between the output power of the turbine and the compression power of the compressor. At the low range of engine speed, the exhaust energy is insufficient, and therefore the power improvement of the IBC system is lower. It is because that most of the exhaust gas energy is used to boost intake gas, and the compressor and turbine efficiencies are lower under the low mass flow rate at the low range of engine speed. The power improvement is going up with increasing engine speed. Beyond the maximum torque point (RES = 50%), the wastegate of the original turbocharger is gradually open, and the mass flow rate rises. Moreover, the IBC system has an optimal turbocharger speed which influences the expansion and compression work. Figure 5(a) and (b) illustrates the IBC compressor pressure ratio and the turbine expansion ratio at different turbocharger speeds. Both the compressor pressure ratio and the turbine expansion ratio increase with the turbocharger speed rising because both powers of the compressor and the turbine are increasing. Meanwhile, a rising engine speed brings a decreasing compressor pressure ratio and an increasing turbine expansion ratio. The turbine inlet and outlet pressures increase with the engine speed up, which is shown in Figure 6. Taking the models at the low and medium speeds as an example, the efficiency differences are as shown in Figure 7. Compared with the model at low turbocharger speed, the model at the medium speed has higher turbine and compressor efficiencies.

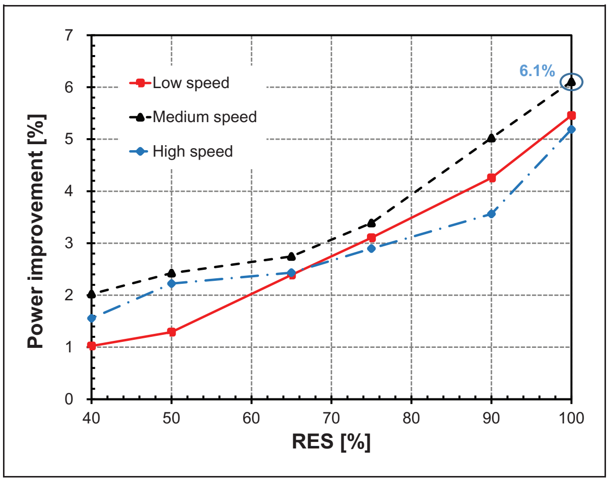

Figure 4. Power improvement of the IBC system at different turbocharger speeds at engine full load operation. RES: relative engine speed.

Compressor efficiency

For the IBC system, the compressor efficiency is a very critical parameter on the system performances.

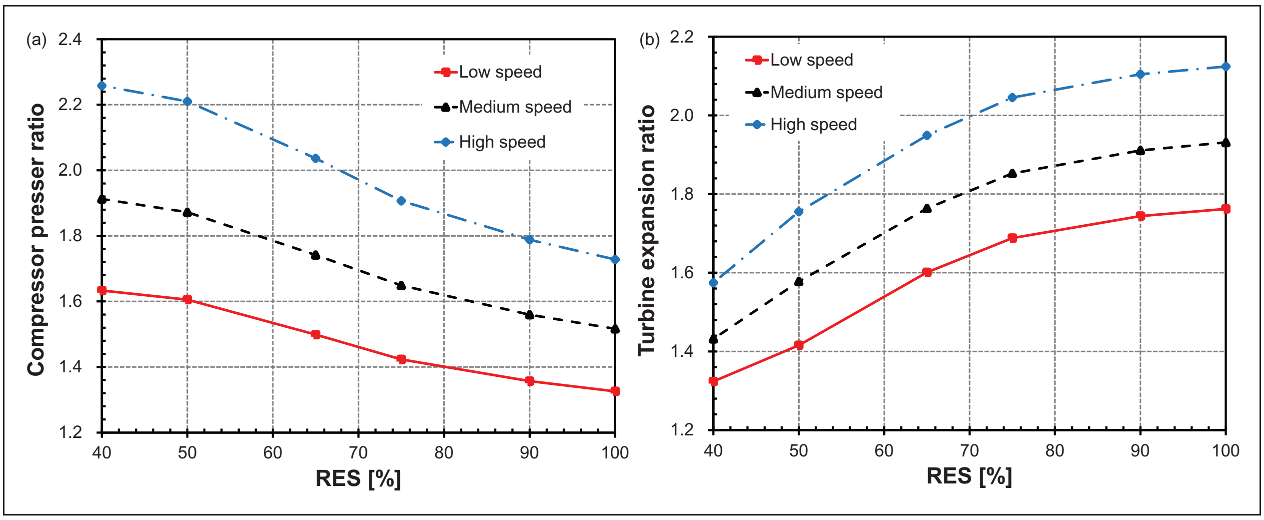

Figure 5. IBC system parameters at different turbocharger speeds: (a) compressor pressure ratio and (b) turbine expansion ratio at engine full load operation. RES: relative engine speed.

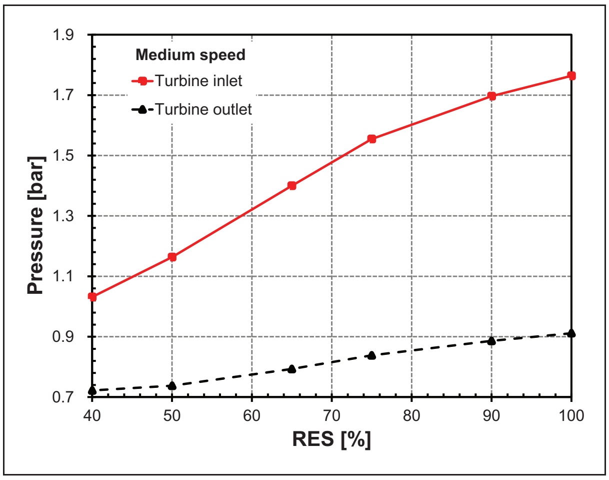

Figure 6. The pressure of IBC turbine inlet and outlet at medium turbocharger speed. RES: relative engine speed.

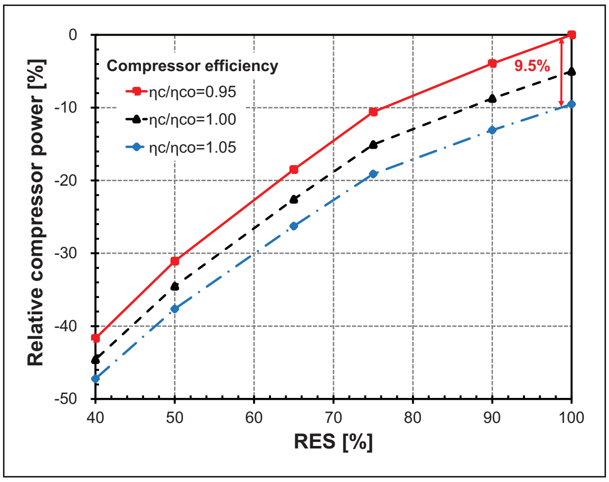

Figure 9. Relative compressor power of the IBC system at different compressor efficiencies. RES: relative engine speed.

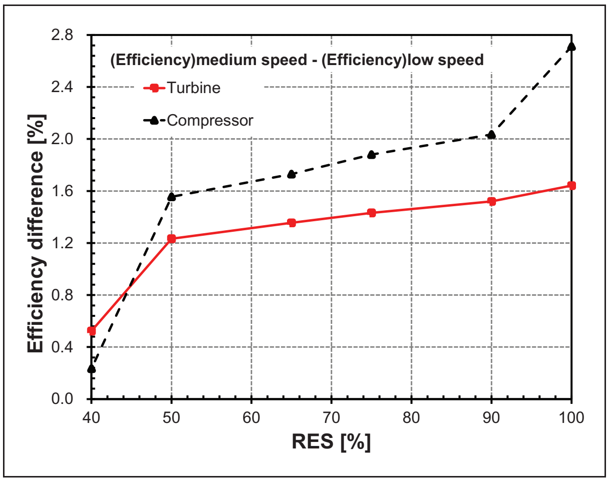

Figure 7. Efficiency differences of IBC turbine and compressor between the medium and low turbocharger speeds. RES: relative engine speed.

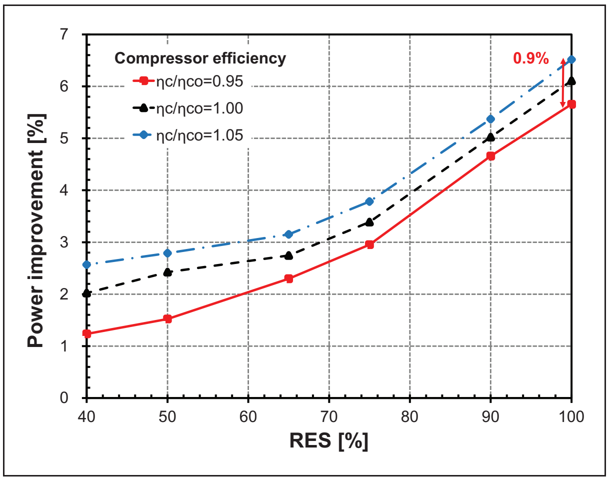

Figure 8. Power improvement of the IBC system at different compressor efficiencies. RES: relative engine speed.

In this part, all models operate at the same turbocharger speed, and only the compressor efficiency is changed. Figure 8 shows different compressor efficiencies. By multiplying the compressor efficiency data with a factor (η_c/η_{c0}) and retaining the mass flow rate and pressure ratio unchanged, three compressor maps with different efficiencies can be obtained. It can be seen that increasing efficiency will bring profits to the system power improvement. They have the same trend versus the engine speed, and the difference value is approximately 0.9% between the two models ($\eta_c/\eta_{c0} = 0.95$ and 1.05) at the rated power point. In the compressor maps, the efficiency difference is about 6.4%, and at low efficiency, the compression power is more when other conditions remain unchanged (Figure 9). It is concluded that 1.0% decline of the compressor efficiency will give an approximately 0.1% loss in the power improvement and a 1.4% increase in the compression power, simultaneously.

Turbine efficiency

Similarly, higher turbine efficiency is always wanted for better engine performances. Keeping all models working at the same turbocharger speed and only altering the turbine efficiency, Figure 10 illustrates the power improvement of the IBC system at different turbine efficiencies. By multiplying the whole efficiency data in the turbine map with a factor (η_t/η_{t0}) and keeping mass flow rate and expansion ratio unchanged, three turbine maps with different efficiencies can be obtained. Conversely, the model with higher efficiency has a better performance at the high range of engine speed. A 1.0% increase in the turbine efficiency will give about 0.2% profit on the improvement of energy recovery in Figure 11, because the efficiency is higher, the turbine output power is more under the same conditions. The output power increases with the engine speed because the exhaust gas has

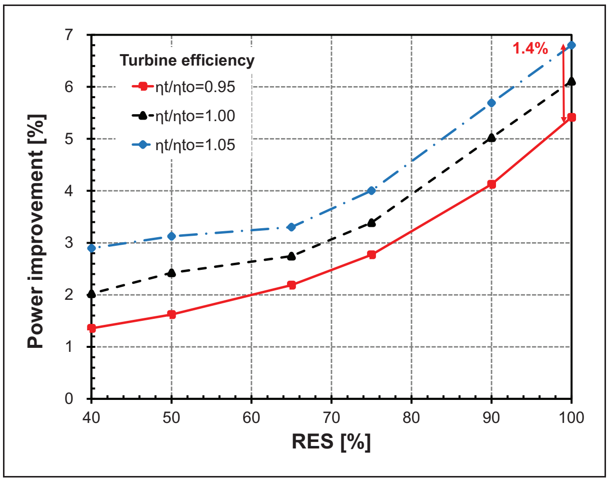

Figure 10. Power improvement of the IBC system at different turbine efficiencies. RES: relative engine speed.

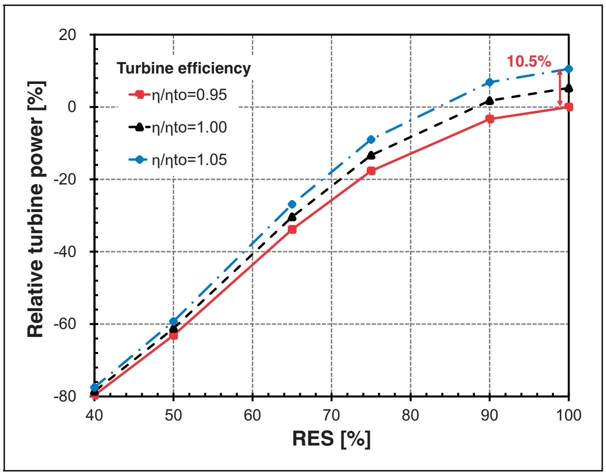

Figure 11. Relative turbine power of the IBC system at different turbine efficiencies. RES: relative engine speed.

higher pressure and temperature. When the turbine efficiency rises by 1.0%, the output power will take an improvement of approximately 1.5%.

Heat exchanger efficiency

The heat exchanger is a crucial component, and its efficiency is a critical parameter in the IBC system. By multiplying the cooling efficiency with a factor ($\varepsilon/\varepsilon_0$) in the heat exchanger model and other conditions remaining same, the power improvement of the IBC system at different heat exchanger efficiencies is shown in Figure 12. The exhaust gas through the turbine still has a high temperature. Therefore, it can be cooled by the heat exchanger, resulting in less compression work in the following compressor. At the whole range of engine speed, the effect laws are similar under different cooling efficiency. In the results, the model ($\varepsilon/\varepsilon_0$=0.95) has a lower efficiency of 8.5% in comparison with the model ($\varepsilon/\varepsilon_0$=1.05), and therefore the results indicate that the system power

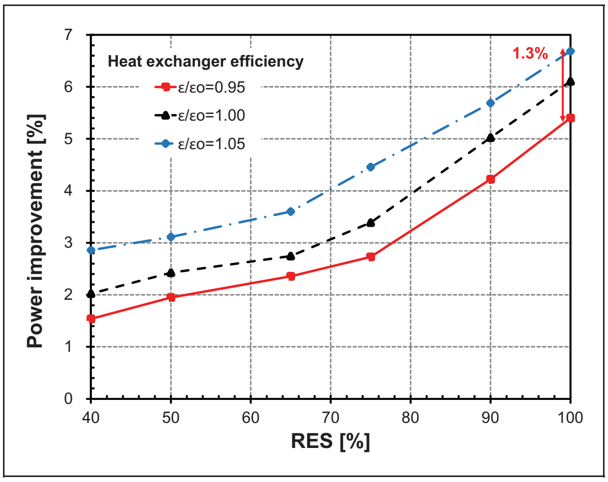

Figure 12. Power improvement of the IBC system at different heat exchanger efficiencies. RES: relative engine speed.

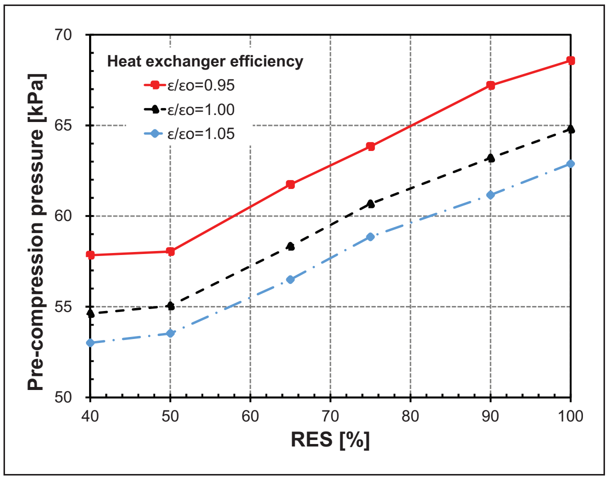

Figure 13. Precompression pressure of the IBC system at different heat exchanger efficiencies. RES: relative engine speed.

improvement will increase by 0.2% if a 1.0% increasing of cooling efficiency is obtained. Meanwhile, the precompression pressure of the IBC system at different heat exchanger efficiencies is shown in Figure 13. With the heat exchanger efficiency increasing, the precompression pressure will decrease, which means that a higher heat exchanger efficiency will increase the turbine expansion ratio and the compressor pressure ratio and a more power improvement will be achieved.

Strategy on improving system revenue

Components' efficiencies

In the sections above, it is clearly demonstrated that components' efficiencies are beneficial when more system power revenues are hoped. At different IBC compressor efficiency factors, the compressor efficiency versus the engine speed at full load is shown in Figure 14. It has been already known that the IBC power improvement difference is approximately 0.9% between the two models (η_c/η_{c0}=0.95 and 1.05) at the rated power point in Figure 8. Figure 14 shows they have a compressor difference of 6.4%. Therefore, the effect of compressor efficiency on the IBC power improvement is small. Moreover, it is very tough to improve turbocharger efficiency. Chen[37] concluded that the compressor efficiency of Rolls-Royce increased by only 10% in about 40 years, and the increasing value was 0.6% in recent 10 years. Not only that, there is usually a trade-off for compressors between a higher efficiency and a wider range of mass flow rate. The ICEs usually work at variable operations, and therefore the system mass flow rate varies widely, which makes it challenging to enhance the turbocharger efficiency.[38] The above also applies to the turbine. The multi-objective optimization of the geometry parameters of the turbine presented that there was a contradiction between turbine efficiency and speed. Pan and Wang[39] used the turbine internal efficiency model to replace the constant entropy efficiency and optimized the wheel diameter ratio, speed ratio, and reaction degree. They found that the internal turbine efficiency depended on the expansion ratio of the rotor and decreased with the increase of the rotor expansion ratio. In consequence, when more turbocharger performances are taken into consideration in the design, enhancing the efficiency is extraordinarily hard.

For the IBC system, heat exchanger represents a significant share of the total module cost. Their optimization should, therefore, be carefully performed. It contributes to the reduction in power consumption, as does the use of a variable speed compressor.[40] Fundamental characteristic regarding heat transfers is the efficiency, and each heat exchanger in the cycle is sized according to this parameter.[16] Hence, the effect of the geometry on the dynamic response of the system is an important aspect and is the main focus.[41] The air-cooler and intercooler of coolant liquid usually have different cooling capacities, and the efficiency values are 60–75 and 80–95%, respectively. As a result, the optimum circuit length is much bigger for the gas cooler than intercooler.[42] Summarily, it is very important to choose a more effective heat exchanger for the improvement of energy recovery.

System matching

When enhancing components' efficiencies is very difficult, the better matching between the components and systems should be pursued. The IBC system has varied inlet conditions with the operations of the engine and the actual components' efficiencies will be changed. The system matching means making the exhaust energy better distributed between the turbocharging turbine and the IBC system turbine, which is mainly dependent on the throat areas of the two turbines.

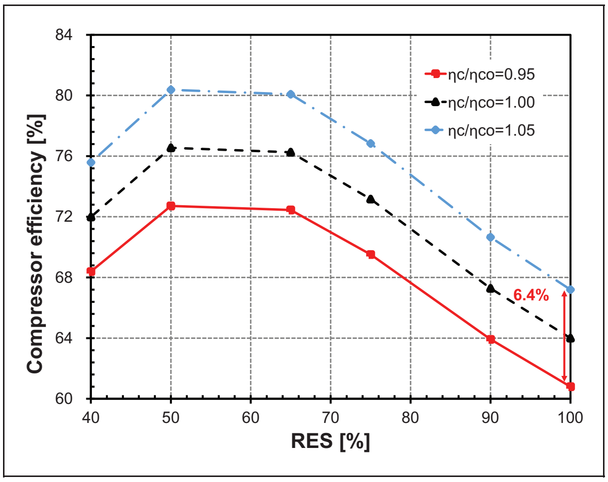

Figure 14. IBC system compressor efficiency at different efficiency factors. RES: relative engine speed.

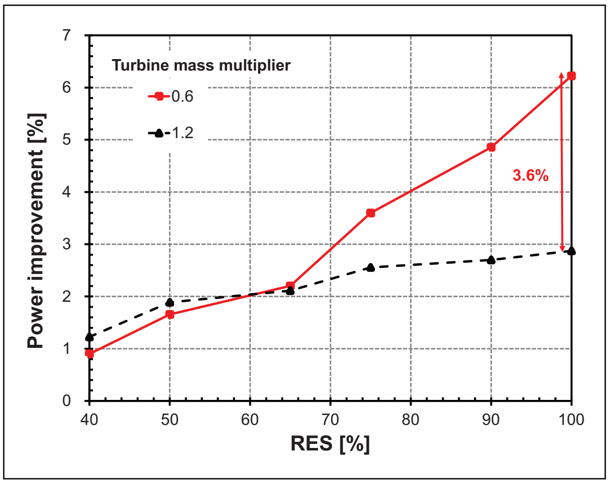

Figure 15. IBC system power improvement at different turbine mass multipliers. RES: relative engine speed.

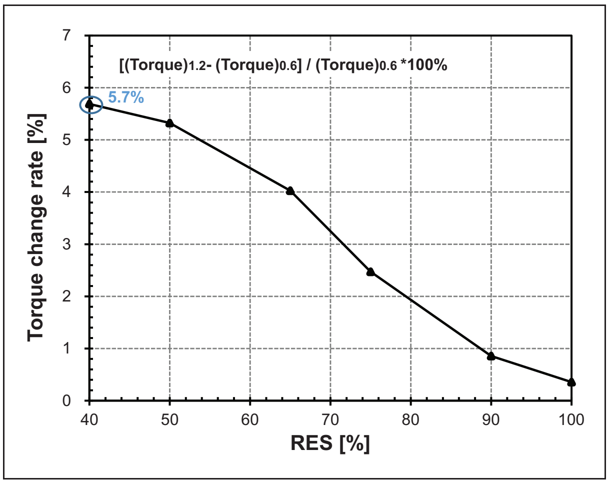

Figure 16. Engine torque change rate at different turbine mass multipliers. RES: relative engine speed.

By multiplying the turbine mass multiplier in the turbine model and keeping other conditions same, the power improvement of the IBC system and the engine torque difference at different turbine mass multipliers are shown in Figures 15 and 16, respectively. It can be seen that the turbine mass multiplier has excellent effects on system performances. At the low range of engine speed, the boost pressure is insufficient, and the engine maximum torque is always hoped, and therefore the turbine of the IBC system should have a large throat area, resulting in more energy for the turbocharging turbine. The engine torque difference maximizes to 5.7% as shown in Figure 16. Conversely, beyond the maximum torque point, the wastegate of the turbocharging turbine is gradually open, and the boost energy is enough. Hence, the IBC turbine with a smaller throat area can be allocated to more exhaust energy. Naturally, it has more power improvement, and the maximum value is 3.4% larger at the rated power point. The matching is very significant, and according to different engine operations, the IBC turbine should have different throat areas. Therefore, VGTs are very acceptable in IBC systems for better matching.

Conclusions and remarks

The IBC has great potential for waste heat energy recovery. To exploit its potential, this study investigates the influences of the system critical parameters on engine power performances under varied engine operations and points its development direction to gain more improvements for the engine exhaust energy recovery. The conclusions are drawn as follows:

1. The IBC system has different power improvements with varying engine operations. The power improvements are gained with the increasing engine speed and it maximizes to 6.1% at the rated power point.
2. The paper sets the influence laws of the turbine and compressor efficiencies in the IBC system. Their increasing of 1.0% will bring the power improvements of approximately 0.2 and 0.1%, respectively. For the energy recovery, enhancing turbocharger efficiencies has low profits and meanwhile, it is very challenging.
3. In the IBC system, higher heat exchanger efficiency means lower compression work. The efficiencies have a considerable difference of approximately 20% between different air-coolers and intercoolers, which will give an energy recovery rate gain of about 3.0%. It is essential to choose a more effective heat exchanger for the improvement of energy recovery.
4. The matching between the IBC system and the turbocharged engine system is very critical. At the low range of engine speed, the turbine of the IBC should have a large throat area to provide enough boost pressure, and the throat area should taper off with the engine speed increasing to achieve more energy recovery. In the future, VGTs are very appropriate for the IBC system.

The IBC system is an effective technology for exhaust energy recovery in ICEs. This work can present the strategy on performance improvement of the IBC system for energy recovery in turbocharged diesel engines. The matching between the systems will be considered and further studied to achieve more significant improvements for energy recovery.

Declaration of Conflicting Interests

The author(s) declared no potential conflicts of interest with respect to the research, authorship, and/or publication of this article.

Funding

The author(s) disclosed receipt of the following financial support for the research, authorship, and/or publication of this article: This research was supported by the National Natural Science Foundation of China (Grant No. 51876097).

ORCID iD

Xinqian Zheng https://orcid.org/0000-0003-1765-0416

References

1. Kai M, Al-Abdullah M, Alzubail A, et al. Synergistic engine-fuel technologies for light-duty vehicles: fuel economy and greenhouse gas emissions. *Appl Energy* 2017; 208: 1538–1561.
2. Kumar BR and Saravanan S. Effect of iso-butanol addition to diesel fuel on performance and emissions of a DI diesel engine with exhaust gas recirculation. *Proc IMechE, Part A: J Power and Energy* 2016; 230: 112–125.
3. Chiara F and Canova M. A review of energy consumption, management and recovery in automotive systems with considerations on future trends. *Proc IMechE, Part D: J Automobile Engineering* 2013; 227: 914–936.
4. Zhu D and Zheng X. A new asymmetric twin-scroll turbine with two wastegates for energy improvements in diesel engines. *Appl Energy* 2018; 233: 263–272.
5. Fennell D, Arellano JMH, Tsolakis A, et al. On-board thermochemical energy recovery technology for low carbon clean gasoline direct injection engine powered vehicles. *Proc IMechE, Part D: J Automobile Engineering* 2018; 232: 1079–1091.
6. Yu C and Chau KT. Thermoelectric automotive waste heat energy recovery using maximum power point tracking. *Energy Convers Manage* 2009; 50: 1506–1521.
7. Kunt MA. An experimental investigation of exhaust waste heat recycling by thermoelectric generators under different thermal conditions for internal combustion engines. *Proc IMechE, Part D: J Automobile Engineering* 2018; 232(12): 1648–1653.
8. Iniesta C, Olazagoitia JL, Viñolas J, et al. Review of travelling-wave thermoacoustic electric-generator technology. *Proc IMechE, Part A: J Power and Energy* 2018; 237(7): 940–957.

9. In BD and Lee KH. A study of a thermoelectric generator applied to a diesel engine. *Proc IMechE, Part D: J Automobile Engineering* 2016; 230: 133–143.
10. Kim TY and Kim J. Assessment of the energy recovery potential of a thermoelectric generator system for passenger vehicles under various drive cycles. *Energy* 2018; 143: 363–371.
11. Jaworski M, Bednarczyk M and Czachor M. Experimental investigation of thermoelectric generator (TEG) with PCM module. *Appl Therm Eng* 2016; 96: 527–533.
12. Leong KY, Saidur R, Kazi SN, et al. Performance investigation of an automotive car radiator operated with nanofluid-based coolants (nanofluid as a coolant in a radiator). *Appl Therm Eng* 2010; 30: 2685–2692.
13. Saidur R, Leong KY and Mohammad HA. A review on applications and challenges of nanofluids. *Renew Sustain Energy Rev* 2011; 15: 1646–1668.
14. Zywica G, Kaczmarczyk TZ and Ihnatowicz E. A review of expanders for power generation in small-scale organic Rankine cycle systems: performance and operational aspects. *Proc IMechE, Part A: J Power and Energy* 2016; 230: 669–684.
15. Glover S, Douglas R, Glover L, et al. Preliminary analysis of organic Rankine cycles to improve vehicle efficiency. *Proc IMechE, Part D: J Automobile Engineering* 2014; 228: 1142–1153.
16. Chen H, Goswami DY and Stefanakos EK. A review of thermodynamic cycles and working fluids for the conversion of low-grade heat. *Renew Sustain Energy Rev* 2010; 14: 3059–3067.
17. Dolz V, Novella R, García A, et al. HD diesel engine equipped with a bottoming Rankine cycle as a waste heat recovery system. Part 1: study and analysis of the waste heat energy. *Appl Therm Eng* 2012; 36: 269–278.
18. Wang E, Yu Z, Zhang H, et al. A regenerative supercritical-subcritical dual-loop organic Rankine cycle system for energy recovery from the waste heat of internal combustion engines. *Appl Energy* 2017; 190: 574–590.
19. Quoilin S, Broek MVD, Declaye S, et al. Techno-economic survey of organic rankine cycle (ORC) systems. *Renew Sustain Energy Rev* 2013; 22: 168–186.
20. Zhu D and Zheng X. Asymmetric twin-scroll turbocharging in diesel engines for energy and emission improvement. *Energy* 2017; 141: 702–714.
21. Hawley JG, Wallace FJ, Cox A, et al. Variable geometry turbocharging for lower emissions and improved torque characteristics. *Proc IMechE, Part D: J Automobile Engineering* 2005; 213: 145–159.
22. Aghaali H and Ångström HE. A review of turbocompounding as a waste heat recoverysystem for internal combustion engines. *Renew Sustain Energy Rev* 2015; 49: 813–824.
23. Mao B, Yao M, Zheng Z, et al. Effects of dual loop EGR and variable geometry turbocharger on performance and emissions of a diesel engine. SAE technical paper 2016-01-2340, 2016.
24. Zamboni G and Capobianco M. Influence of high and low pressure EGR and VGT control on in-cylinder pressure diagrams and rate of heat release in an automotive turbocharged diesel engine. *Appl Therm Eng* 2013; 51: 586–596.
25. Hu Z, Deng K, Cui Y, et al. Steady-state and transient control strategies for a two-stage turbocharged diesel engine. *Proc IMechE, Part D: J Automobile Engineering* 2018; 232(9): 1167–1179.
26. Chen Z, Copeland C, Ceen B, et al. Modeling and simulation of an inverted Brayton cycle as an exhaust-gas heat-recovery system. *J Eng Gas Turbines Power* 2016; 139: 9363.
27. Wilson GD. *The design of high-efficiency turbomachinery and gas turbines*. Boston: MIT Press, 1984.
28. Alabdoadaim MA, Agnew B and Potts I. Examination of the performance of an unconventional combination of Rankine, Brayton, and inverse Brayton cycles. *Proc IMechE, Part A: J Power and Energy* 2006; 6: 305–313.
29. Zhang Z, Chen L and Sun F. Performance optimisation for two classes of combined regenerative Brayton and inverse Brayton cycles. *Int J Solar Energy* 2014; 33: 723–741.
30. Zhang W, Chen L and Sun F. Power and efficiency optimization for combined Brayton and inverse Brayton cycles. *Appl Therm Eng* 2009; 29: 2885–2894.
31. Goodarzi M, Kiasat M and Khalilidehkordi E. Performance analysis of a modified regenerative Brayton and inverse Brayton cycle. *Energy* 2014; 72: 35–43.
32. Giannetti N, Milazzo A and Rocchetti A. Cascade refrigeration system with inverse Brayton cycle on the cold side. *Appl Therm Eng* 2017; 127: 986–995.
33. Chen Z and Copeland CD. Inverted Brayton cycle employment for a highly downsized turbocharged gasoline engine. In: *SAE Int Powertrains Fuels Lubricants Meeting 2015-01-1973*, 2015.
34. Kennedy I, Chen Z, Ceen B, et al. Inverted Brayton cycle with exhaust gas condensation. In: *ASME turbo expo 2017: turbomachinery technical conference and exposition*, Charlotte, NC, USA, 26–30 June 2017, paper no. GT2017-64695.
35. Copeland CD and Chen Z. The benefits of an inverted Brayton bottoming cycle as an alternative to turbo-compounding. In: *ASME turbo expo 2017: turbomachinery technical conference and exposition*, Montréal, Canada, 15–19 June 2015, paper no. GT2015-42623.
36. Zhuge W, Zhang Y, Zheng X, et al. Development of an advanced turbocharger simulation method for cycle simulation of turbocharged internal combustion engines. *Proc IMechE, Part D: J Automobile Engineering* 2009; 223: 661–672.
37. Chen G. Design characteristics of Trent 1000. *Aeroengine* 2009; 4(35): 1–6.
38. Erbaş M and Bıyıkoğlu A. Design and multi-objective optimization of organic Rankine turbine. *Int J Hydrogen Energy* 2015; 40: 15343–15351.

39. Pan L and Wang H. Improved analysis of organic Rankine cycle based on radial flow turbine. *Appl Therm Eng* 2013; 61: 606–615.
40. Ha D and Ji H. Performance characteristics of a combined air conditioner and refrigerator system interconnected via an intercooler. *Int J Refrig* 2015; 49: 57–68.
41. Jiménez-Arreola M, Pili R, Wieland C, et al. Analysis and comparison of dynamic behavior of heat exchangers for direct evaporation in ORC waste heat recovery applications from fluctuating sources. *Appl Energy* 2018; 216: 724–740.
42. Li W. Optimal analysis of gas cooler and intercooler for two-stage CO_2, trans-critical refrigeration system. *Energy Convers Manage* 2013; 71: 1–11.

Appendix

Notation

Subscripts

c	compressor
t	turbine